Small-Angle Neutron Scattering from Elastomeric Networks in which the Junctions Alternate Regularly in their Functionality

Aris Skliros, James E. Mark, Andrzej Kloczkowski*

We compute scattering form factors for SANS from labeled paths in Gaussian phantom networks in which junctions alternate regularly in their functionality (the number of chains emanating from a junction). Our calculations are based on the James-Guth model of rubber-like elasticity, which assumes that fluctuations are strain independent, while mean vectors transform affinely with the applied strain. Kratky plots for scattering from isotropic and uniaxially stretched bifunctional networks are computed and compared with corresponding plots for the simpler unifunctional networks. The results show the effects of the length of the labeled path, extent of deformation, direction of scattering with respect to the principal axis of the deformation and the functionalities of the network junctions.

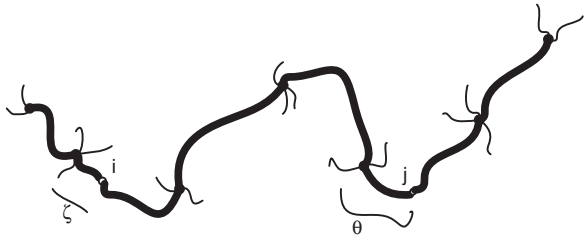

Introduction

The concept of the phantom polymer network in the theory of rubber-like elasticity was first developed over 60 years ago by James and Guth.[1,2] They assumed that polymer chains interact only at junction points (cross-links) and that they may pass freely through one another, that is, they are "phantoms". This phantom approximation neglects inter- (and intra-) chain interactions that lead to entanglements and topological constraints in real polymers. James and Guth also assumed that the distribution of end-to-end vectors of the network chains is Gaussian and is the same before cross-linking and in the cross-linked undeformed network. Additionally, it was assumed that all chains have the same length and that all junctions in the network have the same functionality ϕ (defined as a number of chains connected at each junction or cross-link). They also assumed the network to be composed of two types of junctions: fixed junctions situated on the rubber surface that preserved the volume of the elastomer, and free junctions inside the polymer bulk, fluctuating around their time-averaged mean positions. Additionally, it was assumed that fluctuations of junctions are strain independent while all mean (time-averaged) vectors transform affinely with the applied macroscopic strain.

The idea of the phantom network is very similar to the concept of the ideal gas in the kinetic theory of gases. Just as the ideal gas is a basis for theories of real gases, the phantom network theory provides a foundation for more advanced theories of real networks.

A. Skliros
Department of Biochemistry, Biophysics and Molecular Biology, and L. H. Baker Center for Bioinformatics and Biological Statistics, Iowa State University, Ames, IA 50011-0320, USA
J. E. Mark
Department of Chemistry, University of Cincinnati, Cincinnati, OH 45221-0172, USA
A. Kloczkowski
Department of Biochemistry, Biophysics, and Molecular Biology and L. H. Baker Center for Bioinformatics and Biological Statistics, Iowa State University, Ames, IA 50011-0320, USA
E-mail: kloczkow@iastate.edu

DOI: 10.1002/mats.200900041

The theory of James and Guth has subsequently been reinterpreted and improved by various authors.[3–7] They originally[1,2] assumed that the network had a connectivity of a cubic lattice with many small loops. The later theories[5–7] used the assumption that the network had a topology of a tree, without loops. For a network cross-linked in the undiluted amorphous state, the probability of formation of small loops is rather small, and therefore the assumption of a tree-like structure of the network is reasonable. Pearson[7] was the first to investigate polymer networks at length scales smaller than the end-to-end chain dimensions. He computed the mean-square fluctuations and cross-correlations of fluctuations for points along the chain. This enabled the calculation of fluctuations of mean-square distances between two points, and computation of the scattering form factor for small-angle neutron scattering (SANS) from labeled end-linked chains.[7] Neutron scattering from labeled chains cross-linked into a polymer network was first computed by Warner and Edwards[8] using the replica theory.

Scattering from labeled deuterated chains in mechanically stretched polymer networks allows one to study the behavior of the single network chain upon macroscopic deformation. The first calculation of SANS from such system was done by Benoit et al.[9] They assumed that the end-linked deuterated chain (including all its points along the contour) deforms affinely. Scattering from end-linked deuterated chains in a phantom network was subsequently calculated by Pearson[7] and Ullman.[10] Ullman also studied the scattering from a labeled path with a specified number of cross-links along its contour length.[11] He considered a network to have a tree-like topology and used a simplifying assumption that different chain vectors along that path are uncorrelated. This assumption is, however, not correct, as shown by Kloczkowski, Mark and Erman,[12] who computed the exact scattering form factors for labeled paths within the James and Guth phantom network model.[12] These calculations were based on the exact analytical expressions for the mean-square fluctuations of the distance between two points along a path separated by several junctions derived earlier by Kloczkowski, Mark and Erman.[13] The same problem was also studied independently by Higgs and Ball,[14] using the resistor network method. The calculations of Kloczkowski et al. on chain dimensions and fluctuations in phantom Gaussian networks were later extended to deformed networks,[15] bimodal networks (networks composed of chains of two different lengths),[16] and, most recently, to networks with alternating functionally (a network in which one chain end has functionality ϕ_1, and another end has functionality ϕ_2).[17] In the case of bimodal networks, SANS form factors were also computed.[16] An overview of most of these results is provided elsewhere.[18–20]

In this study, we first briefly review the theory of phantom Gaussian networks and its most recent extension to networks with junctions of alternating functionality. This is followed by a discussion of the theory of neutron scattering from networks in general. We then apply the SANS theory to networks with alternating functionality and compare small-angle neutron scattering from labeled end-linked and cross-linked chains in such networks, with scattering from regular networks having constant functionality. Finally we discuss possible synthesis of the proposed random polymer networks with alternating functionally for experimental testing of these theoretical predictions.

Model Used in Calculations

Figure 1 shows a long labeled (deuterated) path, represented by a bold line, cross-linked into a polymer network. The cross-links which connect the labeled path to the network are represented by large dots. The unlabeled chains cross-linked to the path are denoted by light lines. We assume that the deuterated path consists of n chains of equal length. There are $n-1$ junctions along the path (if we exclude the two terminal ones) out of which n_1 have functionality ϕ_1 and n_2 have functionality ϕ_2. Since one end of the chain always has functionality ϕ_1 and another end has functionality ϕ_2, the functionalities of junctions along the path alternate regularly. We assume that there are N scattering centers along the full path, evenly distributed on each chain. Without loss of generality, we assume the absence of dangling chains at the ends of the path. The two points i and j shown in Figure 1 represent the two scattering centers. The quantities ζ and θ represent, respectively, the fractional distances of the positions of centers i and j relative to the nearest cross-link to the left of each, measured as the ratio of the contour length of the chain between point i (or j) and the closest cross-link on the left, to the total length of the chain. From this definition it follows that $0 \leq \zeta, \theta \leq 1$.

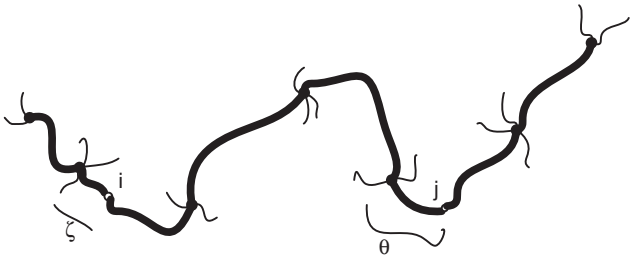

Figure 1. Labeled path in a cross-linked network. The fractional distances z and θ of two points i and j along the path with respect to their nearest cross-links on the left are shown. There are d junctions separating points i and j.

Macromol. Theory Simul. **2009**, *18*, 537–544

Macromolecular Journals
DOI: 10.1002/mats.200900041

We assume that the distribution function of the vector $\mathbf{r}_{ij}$ between two scattering centers i and j in the undeformed state is Gaussian:

$$\Omega_0(r_{ij}) = \left(\frac{3}{2\pi\left\langle r_{ij}^2\right\rangle_0}\right)^{\frac{3}{2}} \exp\left(\frac{-3r_{ij}^2}{2\left\langle r_{ij}^2\right\rangle_0}\right) \tag{1}$$

where $\left\langle r_{ij}^2\right\rangle_0$ is the mean-square distance between points i and j in the undeformed state. The subscript 0 denotes the undeformed state. For the deformed state the distribution function is given by the equation

$$\begin{aligned}\Omega(r_{ij}) = &\left[(2\pi)^3\left\langle x_{ij}^2\right\rangle\left\langle y_{ij}^2\right\rangle\left\langle z_{ij}^2\right\rangle\right]^{-1/2} \\ &\exp\left(-x_{ij}^2/2\left\langle x_{ij}^2\right\rangle - y_{ij}^2/2\left\langle y_{ij}^2\right\rangle - z_{ij}^2/2\left\langle z_{ij}^2\right\rangle\right)\end{aligned} \tag{2}$$

where $\left\langle x_{ij}^2\right\rangle, \left\langle y_{ij}^2\right\rangle, \left\langle z_{ij}^2\right\rangle$ are the mean squares of the three components of the vector $\mathbf{r}_{ij}$ in the deformed state.

In order to calculate the scattering form factor $S(\mathbf{q})$ from the labeled path in the network we take the Fourier Transform of the distribution function $\Omega(r_{ij})$ averaged over all pairs of scattering centers along the path as:

$$S(q) = \frac{1}{N^2}\sum_{i=1}^{N}\sum_{j=1}^{N}\int e^{i\mathbf{q}\cdot\mathbf{r}_{ij}}\Omega(r_{ij})\ d\mathbf{r}_{ij} \tag{3}$$

The quantity $\mathbf{q}$ is the scattering vector representing the difference between the incident and scattered wave vectors, $\mathbf{k}_0$ and $\mathbf{k}$, respectively, and $q = (4\pi/\lambda)\ \sin\ (\theta/2)$. Here θ is the scattering angle and λ is the wavelength of radiation. Substituting Equation (2) into (3) leads to:

$$S(q) = \frac{1}{N^2}\sum_{i=1}^{N}\sum_{j=1}^{N}\exp\left(-q_x^2\left\langle x_{ij}^2\right\rangle/2 - q_y^2\left\langle y_{ij}^2\right\rangle/2 - q_z^2\left\langle z_{ij}^2\right\rangle/2\right) \tag{4}$$

where q_x, q_y, q_z are the components of the vector $\mathbf{q}$. We can write the vector $\mathbf{r}_{ij}$ as

$$\mathbf{r}_{ij} = \bar{\mathbf{r}}_{ij} + \Delta\mathbf{r}_{ij} \tag{5}$$

where $\bar{\mathbf{r}}_{ij}$ is the time average of $\mathbf{r}_{ij}$ and $\Delta\mathbf{r}_{ij}$ is the instantaneous fluctuation of $\mathbf{r}_{ij}$ from the mean $\bar{\mathbf{r}}_{ij}$. Additionally we have,

$$\left\langle r_{ij}^2\right\rangle = \left\langle \bar{r}_{ij}^2\right\rangle + \left\langle (\Delta r_{ij})^2\right\rangle \tag{6}$$

since the directions of instantaneous fluctuations with respect to $\bar{\mathbf{r}}_{ij}$ are uncorrelated. Additionally, since mean-square fluctuations are strain independent, while the mean vectors deform affinely with the applied external strain, we have:

$$\begin{aligned}\left\langle \bar{x}_{ij}^2\right\rangle &= \lambda_x^2\left\langle \bar{x}_{ij}^2\right\rangle_0 \\ \left\langle (\Delta x_{ij})^2\right\rangle &= \left\langle (\Delta x_{ij})^2\right\rangle_0\end{aligned} \tag{7}$$

with similar expressions for the y and z components. In Equation (7), λ_x represents the x-component of the principal deformation gradient tensor $\boldsymbol{\lambda}$ defined as:

$$\lambda = \begin{bmatrix}\lambda_x & 0 & 0\\ 0 & \lambda_y & 0\\ 0 & 0 & \lambda_z\end{bmatrix} \tag{8}$$

where $\lambda_x, \lambda_y, \lambda_z$ represent the ratios of the final dimensions of the network to the corresponding dimensions in the state of reference. Equation (7) may be rewritten as:

$$\begin{aligned}\left\langle \bar{x}_{ij}^2\right\rangle &= \lambda_x^2\left\langle \bar{x}_{ij}^2\right\rangle_0 + \left\langle (\Delta x_{ij})^2\right\rangle_0 \\ &= \left[\lambda_x^2 + \left(1-\lambda_x^2\right)\frac{\left\langle (\Delta x_{ij})^2\right\rangle_0}{\left\langle x_{ij}^2\right\rangle_0}\right]\left\langle x_{ij}^2\right\rangle_0\end{aligned} \tag{9}$$

For the undeformed random coil chain we have:

$$\left\langle r_{ij}^2\right\rangle_0 = \eta\left\langle r^2\right\rangle_0 \tag{10}$$

Here $\eta = \frac{|i-j|}{N_0}$ represents the ratio of the length of the contour path between points i and j to the total length of the single chain (composed of N_0 segments).

The state of macroscopic deformation for uniaxial tension in the x-direction is expressed as:

$$\lambda = \begin{bmatrix}\lambda_{\|} & & \\ & \lambda_{\perp} & \\ & & \lambda_{\perp}\end{bmatrix} = (v_{20}/v_2)^{1/3}\begin{bmatrix}\alpha & & \\ & \alpha^{-1/2} & \\ & & \alpha^{-1/2}\end{bmatrix} \tag{11}$$

where the subscripts $_{\perp}$ and $_{\|}$ refer to directions perpendicular and parallel to the direction of stress, respectively, α is the ratio of final length to initial, swollen but undistorted length of the rubber network, and v_{20} and v_2 are polymer volume fractions in the network in the reference state and during the stretching experiment, respectively. The general formula for the scattering form factor $S(q)$ for uniaxial tension derived from Equation (3) and (9) is:[12]

$$\begin{aligned}S(q) = &\frac{1}{n^2}\sum_{n_i=1}^{n}\sum_{n_j=1}^{n}\int_0^1 d\theta\int_0^1 d\varsigma \\ &\exp\left\{-\nu_{\|}\left[\lambda_{\|}^2|n_j+\theta-n_i-\varsigma| + \left(1-\lambda_{\|}^2\right)\left[\left\langle (\Delta r_{ij})^2\right\rangle\right]\right]\right\}\end{aligned} \tag{12}$$

with $\nu_{||}$ defined as:

$$\nu_{||} = q_{||}^2 < r^2 >_0 /6 \tag{13}$$

The summation in Equation (12) is now carried out over n chains along the path, while the summations over scattering centers within a chain have been replaced by integrals.

Analytical formulas for the mean-square fluctuations $\left\langle \left(\Delta r_{ij}\right)^2 \right\rangle_0$ of the distance between points i and j for a phantom Gaussian network with alternating functionalities of junctions have been derived by us in a recent publication.[17] We used the following formula to compute these fluctuations:

$$< (\Delta r_{ij})^2 >_0 = < (\Delta \mathbf{R}_i - \Delta \mathbf{R}_j)^2 > = < (\Delta R_i)^2 > + < (\Delta R_j)^2 > -2 < \Delta \mathbf{R}_i \cdot \Delta \mathbf{R}_j > \tag{14}$$

Here, $< (\Delta R_i)^2 >$ denotes the mean-square fluctuations of position of point i in the network, and $< \Delta \mathbf{R}_i \cdot \Delta \mathbf{R}_j >$ denotes correlations between instantaneous fluctuations of points i and j. All these quantities were recently computed by us for phantom Gaussian network with alternating functionally.[17] Since the computations leading to these formulas are tedious and lengthy; here we use only the final results; details are provided elsewhere. [17]

The most general solution for the mean-square fluctuations $\left\langle \left(\Delta r_{ij}\right)^2 \right\rangle_0$ of the distance between two points i and j separated by several multifunctional junctions with alternating functionality depends on the functionality of the junctions that are the closest to the left for points i and j. There are four possible cases: i) both of these junctions have functionality ϕ_1, ii) the junction closest to the left for point i has functionality ϕ_1 and closest to the left for point j has functionality ϕ_2, iii) both of them have functionality ϕ_2, and, iv) the junction closest to the left for point i has functionality ϕ_2 and closest to the left for point j has functionality ϕ_1. Each of these four cases has a slightly different solution:

i) If the closest multifunctional junctions on the left of both points i and j are ϕ_1-functional then:

$$\left\langle \left(\Delta r_{ij}\right)^2 \right\rangle_0 = \left\{ 2\frac{\phi_2(\phi_1-1)}{\phi_1(\phi_1\phi_2-\phi_1-\phi_2)} + \frac{(\zeta-\zeta^2+\theta-\theta^2)(\phi_1\phi_2-\phi_1-\phi_2)+(\zeta+\theta)(\phi_1-\phi_2)}{\phi_1\phi_2} - 2\frac{\left[(\zeta)\frac{\phi_1\phi_2-\phi_1-\phi_2}{\phi_2}+1\right]\left[(1-\theta)\frac{\phi_1\phi_2-\phi_1-\phi_2}{\phi_1}+1\right]}{(\phi_1\phi_2-\phi_1-\phi_2)(\phi_1-1)^{d_1}(\phi_2-1)^{d_2}} \right\} < r^2 >_0 \tag{15}$$

where d_1 and d_2 are the numbers of ϕ_1-functional and ϕ_2-functional junctions along the path, respectively, and $< r^2 >_0$ is the mean-square end-to-end vector for polymer chains between multifunctional cross-links. Additionally, in this case we have $d_1 = d_2$.

ii) If the closest multifunctional junction on the left of point i is ϕ_1-functional and on the left of point j is ϕ_2-functional then:

$$\left\langle \left(\Delta r_{ij}\right)^2 \right\rangle_0 = \left\{ \frac{\phi_2^2\phi_1+\phi_1^2\phi_2-\phi_1^2-\phi_2^2}{\phi_1\phi_2(\phi_1\phi_2-\phi_1-\phi_2)} + \frac{(\zeta-\zeta^2+\theta-\theta^2)(\phi_1\phi_2-\phi_1-\phi_2)+(\zeta-\theta)(\phi_1-\phi_2)}{\phi_1\phi_2} - 2\frac{\phi_2}{\phi_1}\frac{\left[(\zeta)\frac{\phi_1\phi_2-\phi_1-\phi_2}{\phi_2}+1\right]\left[(1-\theta)\frac{\phi_1\phi_2-\phi_1-\phi_2}{\phi_2}+1\right]}{(\phi_1\phi_2-\phi_1-\phi_2)(\phi_1-1)^{d_1}(\phi_2-1)^{d_2}} \right\} < r^2 >_0 \tag{16}$$

with $d_1 = d_2 - 1$.

iii) If the closest multifunctional junctions on the left of both points i and j are ϕ_2-functional then:

$$\left\langle \left(\Delta r_{ij}\right)^2 \right\rangle_0 = \left\{ 2\frac{\phi_1(\phi_2-1)}{\phi_2(\phi_1\phi_2-\phi_1-\phi_2)} + \frac{(\zeta-\zeta^2+\theta-\theta^2)(\phi_1\phi_2-\phi_1-\phi_2)+(\zeta+\theta)(\phi_2-\phi_1)}{\phi_1\phi_2} - 2\frac{\left[(\zeta)\frac{\phi_1\phi_2-\phi_1-\phi_2}{\phi_1}+1\right]\left[(1-\theta)\frac{\phi_1\phi_2-\phi_1-\phi_2}{\phi_2}+1\right]}{(\phi_1\phi_2-\phi_1-\phi_2)(\phi_1-1)^{d_1}(\phi_2-1)^{d_2}} \right\} < r^2 >_0 \tag{17}$$

and, similarly to case (i), we have $d_1 = d_2$.

iv) If the closest multifunctional junction on the left of point i is ϕ_2-functional and of the left of point j is ϕ_1-functional then:

$$\left\langle \left(\Delta r_{ij}\right)^2 \right\rangle_0 = \left\{ \frac{\phi_2^2\phi_1+\phi_1^2\phi_2-\phi_1^2-\phi_2^2}{\phi_1\phi_2(\phi_1\phi_2-\phi_1-\phi_2)} + \frac{(\zeta-\zeta^2+\theta-\theta^2)(\phi_1\phi_2-\phi_1-\phi_2)+(\zeta-\theta)(\phi_2-\phi_1)}{\phi_1\phi_2} - 2\frac{\phi_1}{\phi_2}\frac{\left[(\zeta)\frac{\phi_1\phi_2-\phi_1-\phi_2}{\phi_1}+1\right]\left[(1-\theta)\frac{\phi_1\phi_2-\phi_1-\phi_2}{\phi_1}+1\right]}{(\phi_1\phi_2-\phi_1-\phi_2)(\phi_1-1)^{d_1}(\phi_2-1)^{d_2}} \right\} < r^2 >_0 \tag{18}$$

with $d_1 = d_2 + 1$.

The numbers d_1 and d_2 of ϕ_1-functional and ϕ_2-functional junctions satisfy the equation

$$d_1 + d_2 = d \tag{19}$$

where d is the total number of multifunctional junctions between points i and j along the path. Because of this, d is

Macromolecular Journals
DOI: 10.1002/mats.200900041

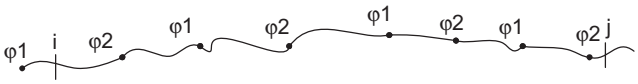

Figure 2. Case where the closest junction on the left of point *i* has functionality ϕ_1, and the closest junction on the left of point *j* has functionality ϕ_2.

always even in cases (i) and (iii), while in cases (ii) and (iv) d is always odd.

During the computation of the scattering form factor from Equation (12) we need to calculate integrals over ζ and θ for varying positions of points i and j along the path, however their location with respect to the closest junctions to the left is determined by indices n_1 and n_2 in double summations in Equation (12). To illustrate this problem let us assume that we want to calculate the contribution to scattering form factor for the case when the closest junction on the left of point i has functionality ϕ_1 whereas the closest junction on the left of point j has functionality ϕ_2, as shown in Figure 2. For this case, $n_i = 1$, $n_j = 8$, and $\left\langle \left(\Delta r_{ij}\right)^2 \right\rangle$ substituted into Equation (12) is given by Equation (16) with $d_1 = 3$ and $d_2 = 4$.

When point i moves to the next chain to the right, as shown in Figure 3 then the corresponding contribution to the scattering form factor in Equation (12) is computed with $n_i = 2$, $n_j = 8$, and fluctuations $\left\langle \left(\Delta r_{ij}\right)^2 \right\rangle$ expressed by Equation (17) with $d_1 = d_2 = 3$, since the closest multifunctional junctions on the left of points i and j both have functionality ϕ_2.

The whole process is continued until all terms in the double sum over n_i, n_j in Equation (12) are included.

Results of Calculations

We made calculations for: a) the nonswollen, uniaxially stretched network; and, b) the isotropic de-swollen network and the de-swollen uniaxially stretched network for five different cases: i) when the functionality of the network has only one value, 3, ii) when the network is bifunctional with functionalities $\phi_1 = 3$, $\phi_2 = 8$, iii) when the network is bifunctional with functionalities $\phi_1 = 3$, $\phi_2 = 4$, iv) when the functionality of the network has only one value, 4, and,v) when the functionality of the network has only one value, 8. A de-swollen network is defined to be a network where the network is formed in a solution and then the solvent is removed or replaced by a smaller amount of

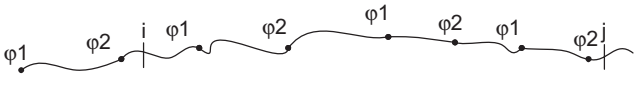

Figure 3. Case where the closest junction on the left of point *i* has functionality ϕ_2, and the closest junction on the left of point *j* has functionality ϕ_2.

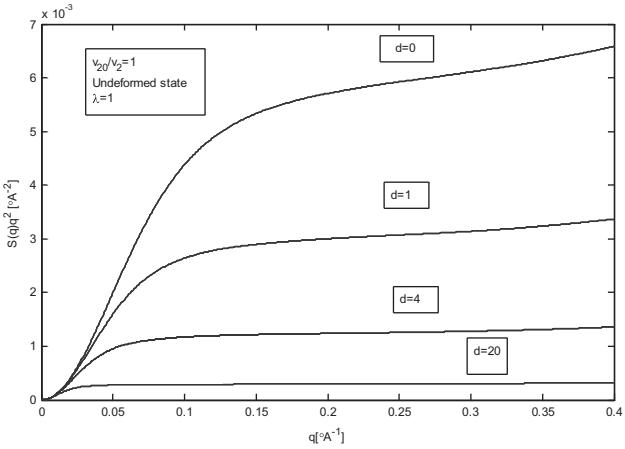

Figure 4. Kratky plot for the nonswollen ($\frac{\nu_{20}}{\nu_2} = 1$), undeformed ($\lambda = 1$) network. The length of the labeled path changes from one chain ($d = 0$ cross-links along the path) up to 21 chains ($d = 20$ cross-links along the path) for the unifunctional cases of $\phi_1 = 3$ and $\phi_2 = 8$ and the bifunctional case of $\phi_1 = 3$, $\phi_2 = 8$. All Kratky plots were calculated as a function of the number d of cross-links along the path. The plots coincide.

another solvent, which means that $\frac{\nu_{20}}{\nu_2} < 1$. There are experimental indications that that for de-swollen networks there is a strong maximum in Kratky plots. In making the computations, we assume that the mean-square end-to-end distance of the equilibrium state is $\langle r^2 \rangle_0 = 2000$ Å.

Figure 4 gives the Kratky plot for the nonswollen ($\frac{\nu_{20}}{\nu_2} = 1$), undeformed ($\lambda = 1$) network. The length of the labeled path changes from one chain ($d = 0$ cross-links along the path) up to 21 chains ($d = 20$ cross-links along the path) for the unifunctional cases of $\phi_1 = 3$, and $\phi_2 = 8$, and the bifunctional case of $\phi_1 = 3$, $\phi_2 = 8$. The Kratky plot was calculated as a function of the number d of cross-links along the path. Since $\lambda = 1$, we see from Equation (1) that for each value of d the three cases $\phi_1 = 3$, $\phi_2 = 8$ and $\phi_1 = 3$, $\phi_2 = 8$ coincide. As was found elsewhere,[1] $q^2S(q)$ decreases as the length of the path (number of cross-links in between) increases.

Figure 5 presents the Kratky plot for the nonswollen ($\frac{\nu_{20}}{\nu_2} = 1$), deformed ($\alpha_{||} = 4$) network for the scattering parallel to the principal axis of deformation for the unifunctional cases of $\phi_1 = 3$ (upper solid line) and $\phi_1 = 8$ (lower solid line) and the bifunctional case of $\phi_1 = 3$, $\phi_2 = 8$ (dashed line). The plot was calculated as a function of the number d of cross-links along the path. This shows the differences between the unifunctional and the bifunctional networks. The ordinate values for the bifunctional network was between the two unifunctional ones up to a certain value of q. The unifunctional network with the smaller functionality has the largest ordinate values.

Figure 6 shows the Kratky plot for the unswollen ($\frac{\nu_{20}}{\nu_2} = 1$), deformed ($\alpha_{vert} = 0.5$) network for the scattering perpendicular to the principal axis of deformation for the unifunc-

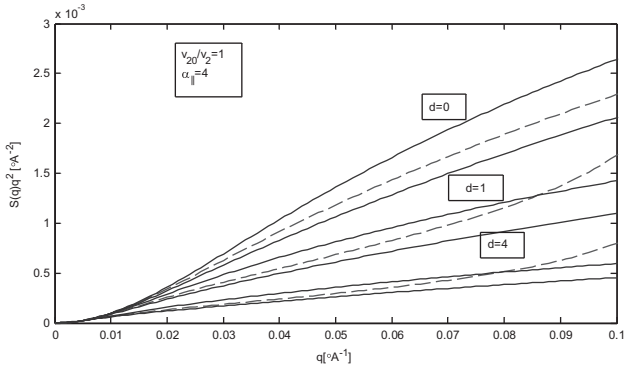

Figure 5. Kratky plot for the unswollen ($\frac{\nu_{20}}{\nu_2} = 1$), deformed ($\alpha_{||} = 4$) network for the scattering parallel to the principal axis of deformation for the unifunctional cases of $\phi_1 = 3$ (upper solid line) and $\phi_2 = 8$ (lower solid line) and the bifunctional case of $\phi_1 = 3,\ \phi_2 = 8$ (dashed line).

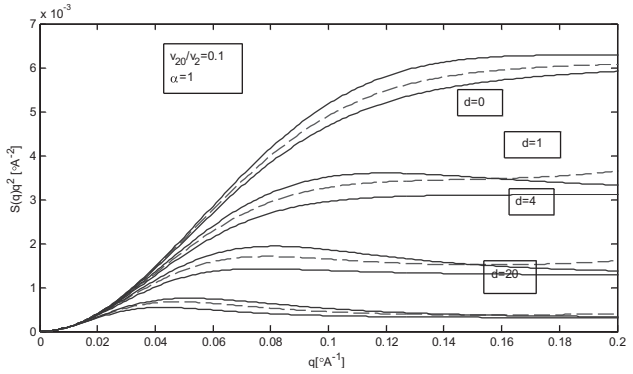

Figure 7. Kratky plot for the isotropically deswollen ($\frac{\nu_{20}}{\nu_2} = 0.1$), ($\alpha = 1$) network for the scattering for the unifunctional cases of $\phi_1 = 3$ (upper solid line) and $\phi_2 = 8$ (lower solid line) and the bifunctional case of $\phi_1 = 3,\ \phi_2 = 8$ (dashed line).

tional cases of $\phi_1 = 3$ (upper solid line) and $\phi_1 = 8$ (lower solid line) and the bifunctional case of $\phi_1 = 3,\ \phi_2 = 8$ (dashed line). We observe a maximum, and also note that the value of q at the maximum decreases as the value of d decreases.

Figure 7 gives the Kratky plot for the isotropically deswollen ($\frac{\nu_{20}}{\nu_2} = 0.1$), ($\alpha = 1$) network for the scattering for the unifunctional cases of $\phi_1 = 3$ (upper solid line) and $\phi_1 = 8$ (lower solid line) and the bifunctional case of $\phi_1 = 3,\ \phi_2 = 8$ (dashed line). We see again the occurrence of maxima, and note that the values for the bifunctional case are between the values of the unifunctional cases.

In Figure 8 we see the Kratky plot for the swollen ($\frac{\nu_{20}}{\nu_2} = 0.2$), uniaxially deformed ($\alpha_{||} = 4$) network for the scattering parallel to the principal axis of deformation for the unifunctional cases of $\phi_1 = 3$ (upper solid line) and $\phi_1 = 8$ (lower solid line) and the bifunctional case of $\phi_1 = 3,\ \phi_2 = 8$ (dashed line). For scattering that is parallel, no maxima are observed.

Figure 9 shows the Kratky plot for the swollen ($\frac{\nu_{20}}{\nu_2} = 0.2$), uniaxially deformed ($\alpha_{vert} = 0.5$) network for the scattering perpendicular to the principal axis of deformation for the unifunctional cases of $\phi_1 = 3$ (upper solid line) and $\phi_1 = 8$ (lower solid line) and the bifunctional case of $\phi_1 = 3,\ \phi_2 = 8$ (dashed line). For this case of perpendicular scattering there are maxima.

Figure 10–15 show the remaining Kratky plots calculated for this study.

Discussion

We have studied a model of polymer networks with alternating functionalities for an infinite network having a tree-like topology and composed of phantom Gaussian chains. In some earlier work,[17] we computed mean-square fluctuations of junctions and points along the chains, and

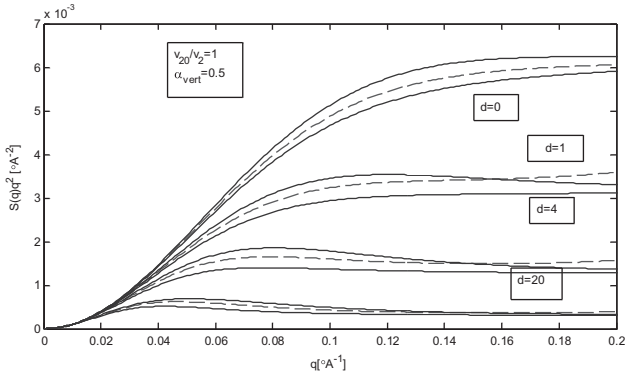

Figure 6. Kratky plot for the nonswollen ($\frac{\nu_{20}}{\nu_2} = 1$), deformed ($\alpha_{vert} = 0.5$) network for the scattering perpendicular to the principal axis of deformation for the unifunctional cases of $\phi_1 = 3$ (upper solid line) and $\phi_2 = 8$ (lower solid line) and the bifunctional case of $\phi_1 = 3,\ \phi_2 = 8$ (dashed line).

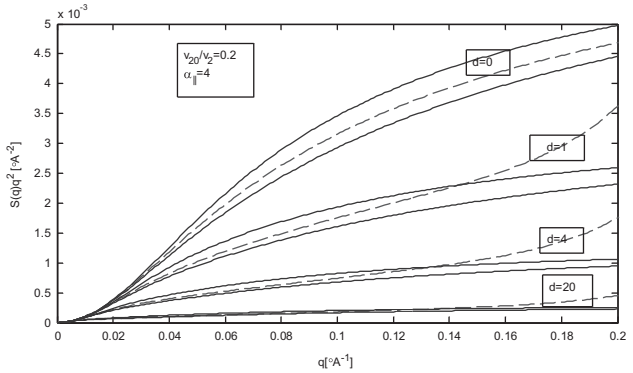

Figure 8. Kratky plot for the swollen ($\frac{\nu_{20}}{\nu_2} = 0.2$), uniaxially deformed ($\alpha_{||} = 4$) network for the scattering parallel to the principal axis of deformation for the unifunctional cases of $\phi_1 = 3$ (upper solid line) and $\phi_2 = 8$ (lower solid line) and the bifunctional case of $\phi_1 = 3,\ \phi_2 = 8$ (dashed line).

Macromol. Theory Simul. **2009**, *18*, 537–544

Macromolecular Journals

DOI: 10.1002/mats.200900041

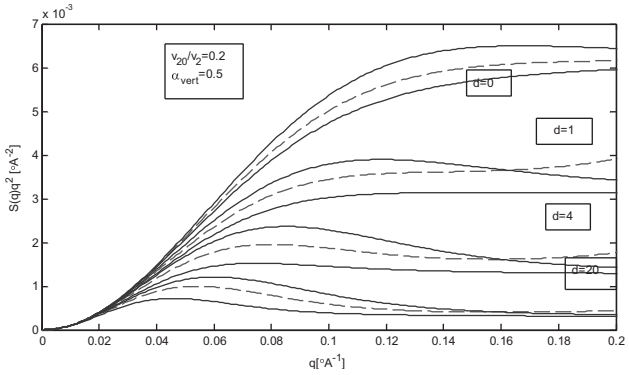

Figure 9. Kratky plot for the swollen ($\frac{\nu_{20}}{\nu_2} = 0.2$), uniaxially deformed ($\alpha_{vert} = 0.5$) network for the scattering perpendicular to the principal axis of deformation for the unifunctional cases of $\phi_1 = 3$ (upper solid line) and $\phi_2 = 8$ (lower solid line) and the bifunctional case of $\phi_1 = 3,\ \phi_2 = 8$ (dashed line).

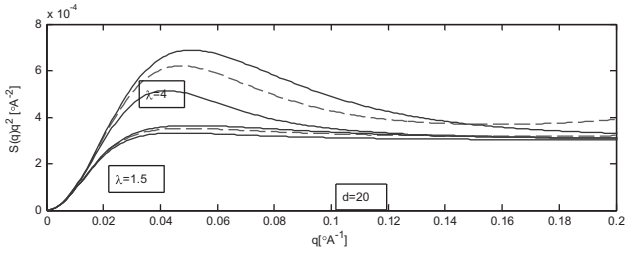

Figure 10. Exact solution of the James-Guth model for a labeled path with $d = 20$ cross-links along the path for the scattering perpendicular to the principal axis of deformation for the non-swollen network for two values of deformation $\lambda = 4 (\alpha_{vert} = 0.5)$ and $\lambda = 1.5 (\alpha_{vert} = \frac{1}{(1.5)^{1/2}})$ for the unifunctional cases of $\phi_1 = 3$ (upper solid line) and $\phi_2 = 8$ (lower solid line) and the bifunctional case of $\phi_1 = 3,\ \phi_2 = 8$ (dashed line).

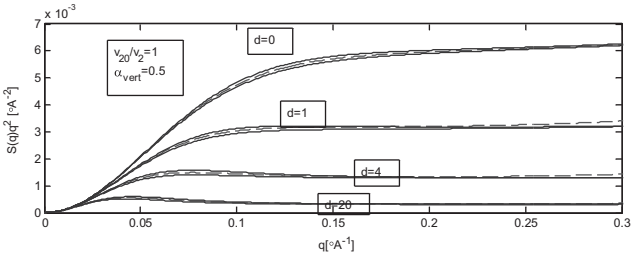

Figure 11. Kratky plot for the nonswollen ($\frac{\nu_{20}}{\nu_2} = 1$), deformed ($\alpha_{vert} = 0.5$) network for the scattering perpendicular to the principal axis of deformation for the unifunctional cases of $\phi_1 = 3$ (upper) and $\phi_2 = 4$ (lower) and the bifunctional case of $\phi_1 = 3,\ \phi_2 = 4$ (dashed line).

correlations between instantaneous fluctuations of two points or junctions, even those separated by other intermediate junctions. In this study, we used these results to compute small-angle neutron scattering from a labeled (deuterated) path containing cross-links in such networks.

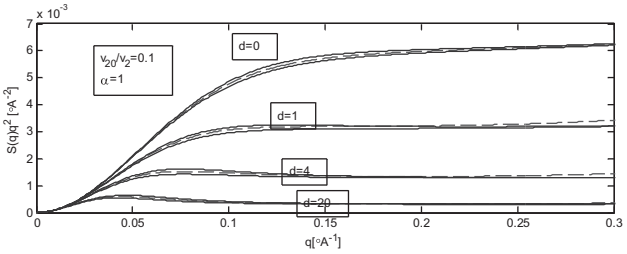

Figure 12. Kratky plot for the isotropically deswollen ($\frac{\nu_{20}}{\nu_2} = 0.1$), ($\alpha = 1$) network for the scattering for the unifunctional cases of $\phi_1 = 3$ (upper) and $\phi_2 = 4$ (lower) and the bifunctional case for $\phi_1 = 3,\ \phi_2 = 4$ (dashed line).

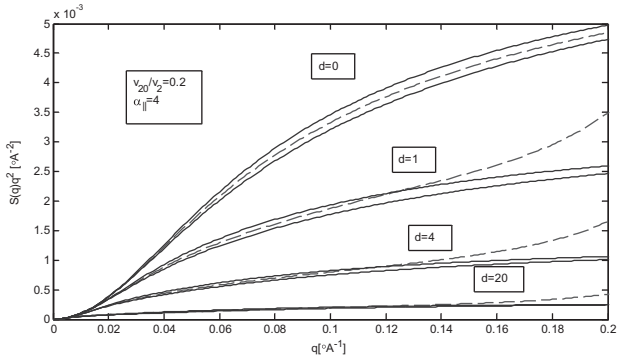

Figure 13. Kratky plot for the swollen ($\frac{\nu_{20}}{\nu_2} = 0.2$), uniaxially deformed ($\alpha_{||} = 4$) network for the scattering parallel to the principal axis of deformation for the unifunctional cases of $\phi_1 = 3$ (upper) and $\phi_2 = 4$ (lower) and the bifunctional case of $\phi_1 = 3,\ \phi_2 = 4$ (dashed line).

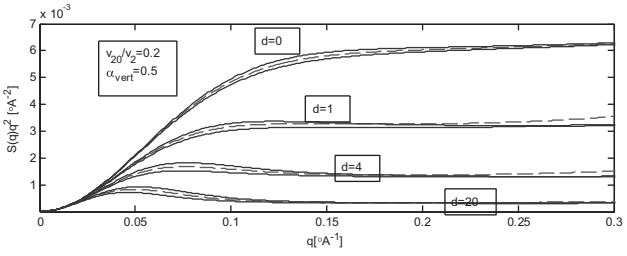

Figure 14. Kratky plot for the swollen ($\frac{\nu_{20}}{\nu_2} = 0.2$), uniaxially deformed ($\alpha_{vert} = 0.5$) network for the scattering perpendicular to the principal axis of deformation for the unifunctional cases of $\phi_1 = 3$ (upper) and $\phi_2 = 4$ (lower) and the bifunctional case of $\phi_1 = 3,\ \phi_2 = 4$ (dashed line).

These new findings enable one to predict the scattering properties of these new bifunctional networks and compare them with regular unifunctional networks. Our work is an example of design of a completely new material based wholly on theoretical principles, specifically with the prediction of physical properties of such a new material prior to its synthesis.

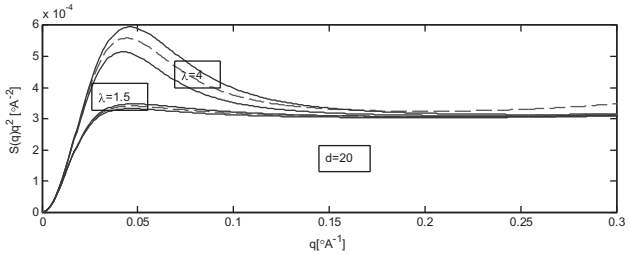

Figure 15. Exact solution of the James-Guth model for a labeled path with $d = 20$ cross-links along the path for the scattering perpendicular to the principal axis of deformation for the unswollen network for two values of deformation $\lambda = 4(\alpha_{vert} = 0.5)$ and $\lambda = 1.5(\alpha_{vert} = \frac{1}{(1.5)^{1/2}})$ for the unifunctional cases of $\phi_1 = 3$ (upper) and $\phi_2 = 4$ (lower) and the bifunctional case of $\phi_1 = 3,\ \phi_2 = 4$ (dashed line).

The preparation of networks with alternating junction functionalities is being currently planned.[25] One promising approach would be the azide–alkyne reactions that have already been used to prepare model networks.[26]

In addition to the scattering properties of the networks studied in this paper we plan to study their scattering using some alternative phantom network models.[27–28] Our future work on these materials will include studies the effects of constraints, due to excluded volume effects and, in fact, such effects in unifunctional networks have been studied by Vilgis and Boue.[29] We also plan to study their elastomeric properties and compare our theoretical predictions with experimental data obtained by mechanical deformations and equilibrium swelling when these new materials became available. For example, it will be of interest to test the prediction that $q^2S(q)$ will show increased values at large values of q, which could correspond to some enhanced ordering at very small length scales.

Acknowledgements: It is a pleasure to acknowledge financial support provided by the *National Institutes of Health* through grants 1R01GM081680, 1R01GM072014, and 1R01GM073095. Also, JEM wishes to acknowledge financial support provided by the *National Science Foundation* through grant DMR-083454 (*Polymers Program, Division of Materials Research*).

Received: June 30, 2009; Published online: November 3, 2009; DOI: 10.1002/mats.200900041

Keywords: elastomers; networks; small-angle neutron scattering (SANS)

[1] H. M. James, *J. Chem. Phys.* **1947**, *15*, 651.
[2] H. M. James, E. Guth, *J. Chem. Phys.* **1947**, *15*, 669.
[3] B. E. Eichinger, *Macromolecules* **1972**, *5*, 496.
[4] P. J. Flory, *Proc. Roy. Soc.* **1976**, *A351*, 351.
[5] W. W. Graessley, *Macromolecules* **1975**, *8*, 186.
[6] W. W. Graessley, *Macromolecules* **1975**, *8*, 865.
[7] D. Pearson, *Macromolecules* **1977**, *10*, 696.
[8] M. Warner, S. F. Edwards, *J. Phys. A: Math. Gen.* **1978**, *11*, 1649.
[9] H. Benoit, R. Duplessix, R. Ober, J. P. Cotton, B. Farnoux, G. Jannick, *Macromolecules* **1975**, *8*, 451.
[10] R. Ullman, *J. Chem. Phys.* **1979**, *71*, 436.
[11] R. Ullman, *Macromolecules* **1982**, *15*, 1395.
[12] A. Kloczkowski, J. E. Mark, B. Erman, *Macromolecules* **1989**, *22*, 4502.
[13] A. Kloczkowski, J. E. Mark, B. Erman, *Macromolecules* **1989**, *22*, 1423.
[14] P. G. Higgs, R. C. Ball, *J. Phys. (Les Ulis, Fr.)* **1988**, *49*, 1785.
[15] B. Erman, A. Kloczkowski, J. E. Mark, *Macromolecules* **1989**, *22*, 1432.
[16] A. Kloczkowski, J. E. Mark, B. Erman, *Macromolecules* **1991**, *24*, 3266.
[17] A. Skliros, J. E. Mark, A. Kloczkowski, *J. Chem. Phys.* **2009**, *130*, 064905.
[18] J. E. Mark, B. Erman, *Rubberlike Elasticity: A Molecular Primer*, Wiley, New York 1988.
[19] B. Erman, J. E. Mark, *Structures and Properties of Rubberlike Networks*, Oxford University Press, New York 1997.
[20] A. Kloczkowski, *Polymer* **2002**, *43*, 1503.
[21] C. Picot, *Prog. Colloid Polym. Sci.* **1987**, *75*, 83.
[22] J. Bastide, J. Herz, F. Boue, *J. Phys. (Les Ulis, Fr.)* **1985**, *46*, 1967.
[23] J. Bastide, *Springer Proceedings in Physics 5*, Springer, New York 1985.
[24] J. Bastide, F. Boue, *Physica* **1986**, *140A*, 251.
[25] J. A. Johnson, J. T. Koberstein, N. J. Turro, A. Skliros, J. E. Mark, A. Kloczkowski, work in progress.
[26] J. A. Johnson, M. G. Finn, J. T. Koberstein, N. J. Turro, *Macromolecules*, **2007**, *40*, 3589.
[27] A. Kloczkowski, J. E. Mark, B. Erman, *Macromolecules* **1992**, *25*, 2455.
[28] A. Kloczkowski, J. E. Mark, B. Erman, *Macromolecules* **1990**, *23*, 1222.
[29] T. Vilgis, F. Boue, *Polymer*, **1986**, *27*, 1154.